Evaluation of the Effects of Dose on Lung Ventilation Calculated from 4D-CT using Deformable Image Registration

An Application of a Ventilation Calculation Algorithm based on 4D-CT

Kujtim Latifi, Thomas J. Dilling, Craig W. Stevens, Vladimir Feygelman,
Eduardo G. Moros and Geoffrey G. Zhang
Department of Radiation Oncology, Moffitt Cancer Center, Tampa, Florida, U.S.A.

Keywords: Deformable Image Registration, Ventilation Calculation, 4D-CT, Lung Ventilation, Radiotherapy, Radiation Dose.

Abstract: Ventilation derived from 4D-CT using deformable image registration (DIR) has been found correlate to the result from a conventional modality very well. How radiation affects ventilation in lungs is still not clearly studied. In this paper, ventilation versus radiation dose is investigated using ΔV method, a ventilation calculation algorithm based on 4D-CT and DIR. Diffeomorphic morphons was used as the DIR tool. Tidal volume normalized ventilation was used in this study. A total of 20 SBRT lung cancer patients' 4D-CT and planning dose data were retrospectively analysed. All the patients had two sets of 4D-CT, one at pre-treatment and one post treatment. Ventilation distributions were calculated based on the two sets of 4D-CT for each case. The two ventilation data sets were aligned using DIR. Radiation dose distributions were resampled to match the resolution of CT images. A ventilation (or ventilation change) and dose values were thus associated to each voxel of the CT images. A function (ventilation change) – dose – volume surface was generated for each case. Average ventilation was found degraded in higher than 20 Gy dose regions for 16 out of the 20 cases. This result can be applied in treatment planning to spare functional lung volumes.

1 INTRODUCTION

Lung functional information has been proposed to be used in radiation therapy (RT) treatment planning to spare normal functional lung volumes (Lavrenkov et al., 2007; Shioyama et al., 2007). Conventionally and clinically, lung functional data are acquired using nuclear medicine techniques (Petersson et al., 2004; Suga, 2002). Recently, algorithms have been developed to derive ventilation distribution matrix from four-dimensional computed tomography (4D-CT) images using deformable image registration (DIR) (Guerrero et al., 2005; Reinhardt et al., 2008; Zhang et al., 2009). Promising comparison result has been made between ventilation images using 4D-CT and a conventional method (Ding et al., 2012). The advantages of ventilation data derived from 4D-CT include its quantitativeness, high resolution and low cost. As 4D-CT is routinely taken for treatment planning purposes when treating lung cancer patients using radiotherapy, ventilation data can be derived from the 4D-CT without any extra imaging procedure.

Functional lung images were suggested to be used in treatment planning to spare functional lung volumes in order to safely escalate radiation dose in patients and improve disease control (Yaremko et al., 2007). However, without a thorough understanding of the effect of radiation dose on lung functions, it is not meaningful setting up objectives or constraints in treatment planning. To meaningfully implement functional lung sparing in treatment planning in clinical practice, a study of ventilation change versus radiation dose needs to be performed.

Ventilation imaging using 4D-CT was proposed to be used to evaluate the ventilation change due to radiation therapy by Ding *et al* in which two patients' data were analysed (Ding et al., 2010). This study uses derived ventilation from 4D-CT scans to evaluate the effects of radiation treatment on lung ventilation. Besides more patient data, a different DIR algorithm and ventilation calculation algorithm were used in this study. In addition, ventilation data

Latifi K., J. Dilling T., W. Stevens C., Feygelman V., G. Moros E. and G. Zhang G..
Evaluation of the Effects of Dose on Lung Ventilation Calculated from 4D-CT using Deformable Image Registration - An Application of a Ventilation Calculation Algorithm based on 4D-CT.
DOI: 10.5220/0004719700050011
In *Proceedings of the International Conference on Bioimaging* (BIOIMAGING-2014), pages 5-11
ISBN: 978-989-758-014-7

in this study were normalized to tidal volume for a more accurate analysis.

2 MATERIALS AND METHODS

The use of patients' de-identified 4D-CT image and 3D dose distribution data in this retrospective study using the ventilation calculation algorithm based on 4D-CT and DIR closely followed an institutional review board (IRB) approved protocol.

Figure 1 shows the flow diagram of the analysis of ventilation change due to radiotherapy using 4D-CT and DIR. Two phases, expiration and inspiration, from each 4D-CT data set were used for ventilation distribution calculation. DIR was applied 3 times for each case, one for each ventilation calculation of the 2 data sets and one to map the 2nd ventilation data (post RT treatment) to the 1st one (pre RT treatment).

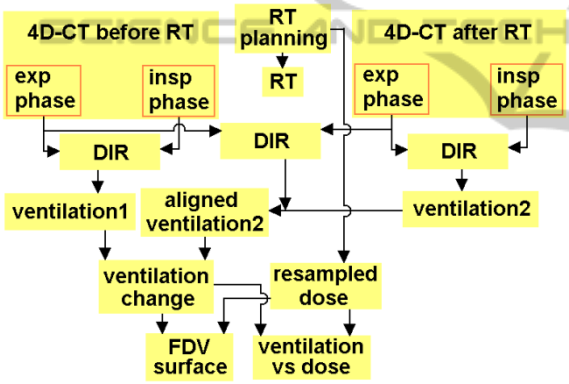

Figure 1: Flow chart of the ventilation change – dose analysis using 4D-CT and DIR. In the diagram, RT = radiation therapy, exp = expiration, insp = inspiration, DIR = deformable image registration, FDV = function (ventilation change) – dose – volume.

The dose distribution from treatment planning usually used 2×2×2 or 3×3×3 mm^3 dose grid. To calculate the function (ventilation change)-dose-volume surface and ventilation change versus dose data, the 3D dose distribution data were resampled to match the CT resolution, usually about 1×1×3 mm^3. The dose distribution was not recalculated in the treatment planning system with the new dose grid size. Linear interpolation was applied in the dose data resampling.

After the DIR and resampling, the two ventilation distributions and thus the ventilation change distribution were aligned with the expiration phase in the pre RT 4D-CT, and so was the dose distribution. The quantitative analysis was based on the aligned distribution data.

2.1 Deformable Image Registration (DIR)

This study uses the diffeomorphic morphons (DM) DIR method (Janssens et al., 2009). In the validation of the DM algorithm, the average target registration error (TRE), for normal end-expiration to end-inspiration registration in a 4D-CT data set, is 1.4±0.6 mm (Latifi et al., 2013c). DM DIR of the normal end-expiration and end-inspiration phases of 4D-CT images was used to correlate the voxels between the two phases.

DM DIR is also used in the 2nd ventilation mapping from the post treatment CT to the pre-treatment CT. After the mapping, the two ventilation data sets are aligned on the pre-treatment CT set. The DIR is performed between the expiration phase of the post treatment 4D-CT and the expiration phase of the pre-treatment 4D-CT. The deformation matrix resulted from the DIR was used to map the ventilation data from the post treatment CT frame to the pre-treatment CT frame.

2.2 Ventilation Calculation

This study uses the ΔV ventilation calculation algorithm (Zhang et al., 2011; Zhang et al., 2009) to derive ventilation from 4D-CT scans.

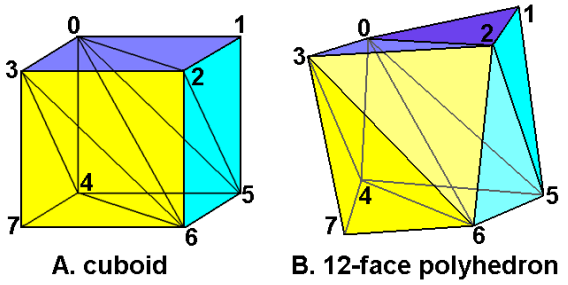

Figure 2: (A) A cuboid can be divided into 6 tetrahedrons. (B) The corresponding 12-face polyhedron (deformed cuboid) is composed of 6 deformed tetrahedrons.

The ΔV method, which is a direct geometrical calculation of the volume change, was used to calculate the local lung expansion or contraction (Zhang et al., 2009). In the expiration phase of a 4D-CT data set, each voxel is a cuboid defined by 8 vertices. In the inspiration phase, this cuboid is changed into a 12-face polyhedron which is still comprised of the corresponding 8 vertices. Any hexahedron or 12-face polyhedron can be divided

into 6 tetrahedrons (Figure 2). The volumes of the cuboid and the 12-face polyhedron (deformed cuboid) are the sums of the volumes of their 6 corresponding tetrahedrons. In the inspiration phase, DIR calculates the corresponding locations of the 8 vertices that define the cuboid in the expiration phase. The volumes of each cuboid and the corresponding deformed cuboid are calculated using the corresponding vertices of each respective polyhedron.

The fundamental volume calculation is based on the volume calculation for each tetrahedron. The coordinates of the 4 vertices of a tetrahedron are used to determine its volume:

$$V = (\boldsymbol{b} - \boldsymbol{a}) \cdot [(\boldsymbol{c} - \boldsymbol{a}) \times (\boldsymbol{d} - \boldsymbol{a})] / 6 \quad (1)$$

where $\boldsymbol{a}$, $\boldsymbol{b}$, $\boldsymbol{c}$, $\boldsymbol{d}$ are the vertices' coordinates expressed as vectors. The volumes of the six tetrahedrons are summed up to generate the volume of the given polyhedron.

The ventilation distribution was calculated as the distribution of

$$P = \Delta V / V_{exp}, \quad (2)$$

where ΔV is the volume change between expiration and inspiration and V_{exp} is the initial volume at expiration (Simon, 2000).

There is often tidal volume (TV) difference between two 4D-CT scans of the same patient. The quantitative ventilation data derived from 4D-CT depends on the TV, since if TV is different, ΔV for each local voxel would be different thus ventilation P is different based on Equation (1). To remove the ventilation dependence on the TV of the patient's respiration, the ventilation change was calculated using the tidal volume normalized ventilation data (Du et al., 2013). Tidal volume is calculated by integrating the local volume change ΔV over the entire lung volume. For two 4D-CT sets, taken before and after treatment, there are two TVs from the ventilation calculations: TV1 from the pre-treatment data set and TV2 from the post-treatment one. In the normalization process, the pre-treatment ventilation distribution is not changed, while the post-treatment ventilation distribution is normalized to TV1 by applying a multiplication factor, TV1/TV2, to every voxel in the lungs. After this normalization, both ventilation data sets have the same tidal volume, TV1, thus removing the final result dependency on the TV. In this study, two sets of ventilation data were compared using this normalization method for each patient.

A reduced lung mask was used in order to avoid any possible artifacts near the lung boundary due to sliding motion (Loring et al., 2005). The margin of the lung mask reduction was 1 mm. The lung masks were automatically generated by density threshold method on the CT images using a homemade computer program.

Ventilation data were calculated and superimposed on the normal end-expiration phase of the 4D-CT before and after RT for each case. DM was also applied to register the two normal end-expiration phases of the 2 sets of 4D-CT, and the resulted deformation matrix was used to deform the ventilation matrix from the after RT data frame to the before RT data frame. The ventilation change distribution was then calculated between the registered ventilation data sets.

Dice similarity coefficient (DSC) index was used to calculate the similarity between the two ventilation volumes (Dice, 1945). When volume A and B are compared, DSC is calculated as

$$DSC(A,B) = \frac{2 \times |A \cap B|}{|A| + |B|} \quad (3)$$

The values of DSC index range between 1.0 and 0.0. A DSC index of 1.0 indicates a complete overlap of the two volumes examined whereas a DSC index of 0.0 indicates no overlap between the volumes examined, and intermediate values describe proportional amount of overlap. To calculate the DSC for the two sets of ventilation data in each case, the ventilation data were converted to relative percentile ventilation distribution (Castillo et al., 2010). Similar to the cumulative dose-volume histogram, if a certain percentage lung volume is covered by a certain ventilation value and below, this ventilation value is converted to the corresponding percentage value of the lung volume in the percentile distribution. The volumes for the DSC index were generated based on the percentile ventilation values. The two aligned ventilation data sets were compared for the similarity of the higher 50% of ventilation volume.

2.3 Patient Data

As 4D-CT is not clinically taken in patient follow-up scans after radiotherapy, patient selection has to be within the group that had second tumor treatment. A 4D-CT is taken for the treatment planning before the second tumor treatment, which can also serve as the follow-up 4D-CT of the first tumor treatment. Among the hundreds of lung cancer patients treated with stereotactic body radiotherapy (SBRT), 20 patients who had second lung tumor treated were selected for this study.

4D-CT sets from before and after RT were used

to derive ventilation for the patients, following an IRB approved protocol. The resolution in the 4D-CT was about 1×1×3 mm^3. All CT data covered the lungs completely. Time between end of treatment and the follow up scan ranged from 1-25 months.

Table 1 lists the statistic data of target volume and dose level volumes in lungs for the 20 patients. Notice that the lung and dose level volumes exclude the gross target volume (GTV). Also, the low dose volumes (<1Gy) were much larger than the high dose volumes (>30Gy, 20~30Gy), usually by 2 orders of magnitude. The internal gross target volume (IGTV) was derived from (at a minimum) the union of the GTV volumes on two extreme phases of the 4D-CT scan and the free breathing scan. The standard IGTV to the planning target volume (PTV) expansion was 5mm axially and 7mm superiorly and inferiorly. The treatment plans were optimized to cover 100% of the IGTV and at least 95% of the PTV by the prescribed dose. Doses ranged from 40-60 Gy delivered in 4-5 fractions.

Table 1: Target volume and dose level volumes in lungs.

Volume	Average	SD	Median	Min	Max
Lung	2447.6	1062.1	2338.7	837.0	4599.6
PTV	34.3	28.2	24.9	5.5	106.7
>30Gy	78.1	85.4	53.5	6.7	359.4
20~30Gy	65.1	66.7	38.2	10.2	276.1
10~20Gy	159.8	128.7	139.4	23.3	536.4
5~10Gy	195.6	145.0	145.6	51.4	589.7
1~5Gy	540.5	436.1	391.2	166.1	1737.5
<1Gy	1402.9	614.6	1372.7	418.5	2778.9

Dose and normalized ventilation were superimposed on the CT volume resulting in each voxel having a volume, normalized ventilation change and a dose and therefore leading to a 3-dimensional histogram, or function (ventilation change) – dose – volume (FDV) surface. An FDV surface was generated for each case based on the aligned data. Accumulating the volumes in different ventilation change ranges in the FDV surface data, 2D dose – volume histograms for the corresponding ventilation change range were generated. Mean TV normalized ventilation within the 1, 5, 10, 20 and 30 Gy regions was calculated before and after RT. The cases were binned into 3 groups with follow-up time of less than 5 months (n = 6), 5 months to 1 year (n = 6) and longer than 1 year (n = 8). The ventilation change versus dose of different follow-up time was compared.

3 RESULTS

Figure 3 shows an example of the dose and calculated ventilation change distributions overlapped on the expiration phase of the 4D-CT. More negative ventilation change, or ventilation degradation, around the tumor (high dose region) can be seen in this example.

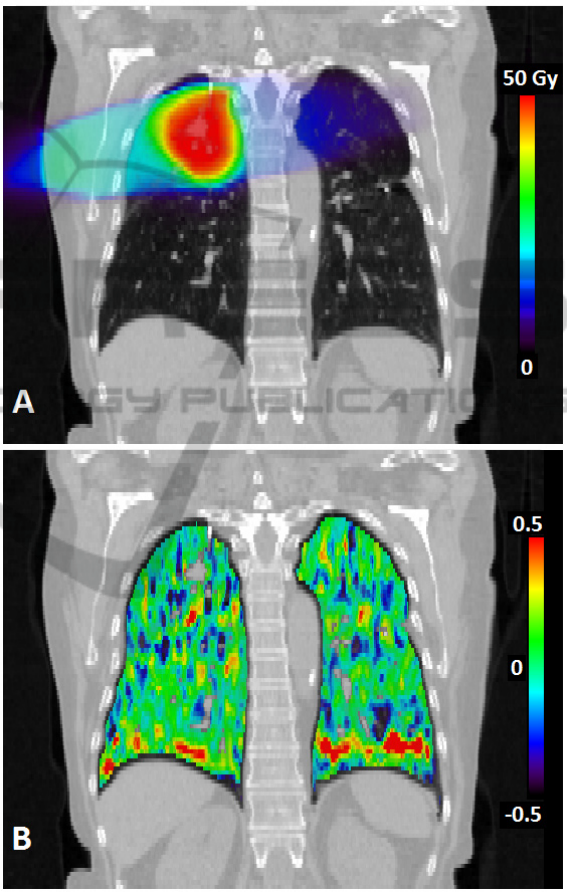

Figure 3: A coronal view of an example of the dose (A) and ventilation change (B) distributions overlapped with the expiration phase of the pre-treatment 4D-CT.

Figure 4 shows a typical FDV surface. Since most of the lung volume is under low dose coverage (Table 1), the surface is peaked close to 0 dose. The maximum value of % volume (vertical axis) in this figure is set at 0.1% to make the high dose surface visible.

Figure 5 shows a typical ventilation change versus dose histogram. For sixteen out of 20 cases, ventilation after treatment was lower within the high dose region compared to that before treatment, which is reflected by the "get worse" curve being

higher than "get better" curve in the high dose region in Figure 5.

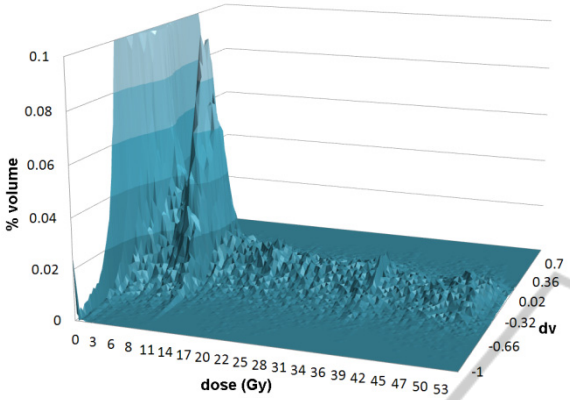

Figure 4: A typical function (ventilation change)-dose-volume (FDV) surface. The volume of the lungs is normalized to 100%. The maximum value of the % volume (vertical axis) is set to 0.1% to make the high dose surface visible. In the figure, dv = ventilation change.

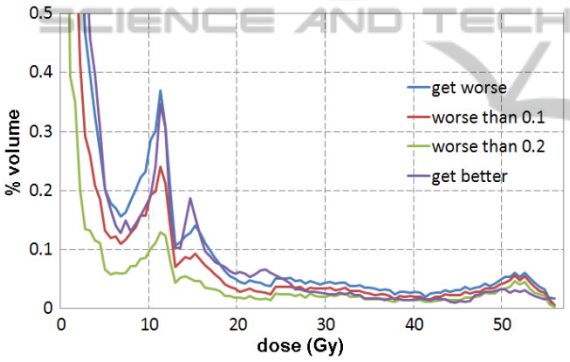

Figure 5: A typical ventilation change versus dose histogram. Curve "get worse" is the volume integration at a certain dose level for lower (worse) ventilation after treatment and "get better" is the volume for higher (better) ventilation. In the figure, worse than 0.1 means the TV normalized ventilation decreased more than 10% after treatment.

Table 2: Ventilation change versus dose over the 20 cases.

Region	Average	SD	Median	Min	Max
<1Gy	0.0002	0.0178	-0.0010	-0.0339	0.0376
1~5Gy	0.0075	0.0365	0.0035	-0.0444	0.1403
5~10Gy	0.0096	0.0522	-0.0004	-0.0427	0.2051
10~20Gy	-0.0074	0.0491	0.0026	-0.1293	0.0764
20~30Gy	-0.0189	0.0664	-0.0091	-0.1805	0.1100
>30Gy	-0.0239	0.0529	-0.0188	-0.0927	0.1448

Figure 6 demonstrates that the trend of the average ventilation change is less dependent on dose. In other words, the average ventilation change versus dose tends to be flattened with time.

Table 2 lists the statistical ventilation change data over the 20 cases. The trend is that the average ventilation degrades with dose when the dose is greater than 20 Gy. The ventilation change difference was statistically significant in the dose regions covered by < 1 Gy and > 30 Gy ($p = 0.006$).

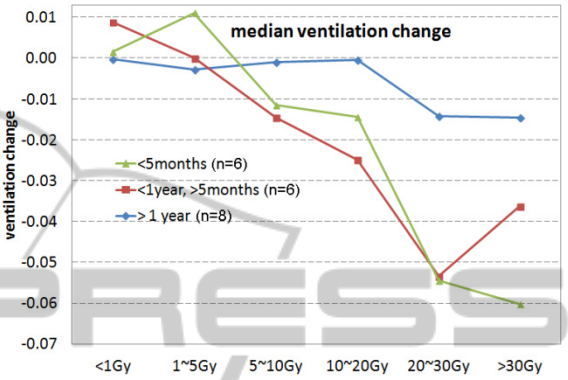

Figure 6: The median values of average ventilation changes in various dose level regions of different groups of follow-up time.

Mean DSC index for the above 50% ventilation volume was 0.60 ± 0.04 (1 SD) with a range 0.52 to 0.69.

For lung tissue regions receiving more than 20 Gy, a decrease in ventilation was observed in 16 of 20 patients. For the 16 cases ventilation within the 20 Gy dose was reduced by an average of 6.4% (range 0.3 to 18.1%). For regions receiving more than 30 Gy, 15 out of 20 patients had an average decrease of ventilation by 4.4% (range 0.6 to 9.3%). Four patients had an average increase of ventilation of 4.1% within the 20 Gy and five patients had an average increase of 3.8% within the 30 Gy region.

4 DISCUSSION

The use of normalized ventilation data in the comparison is to remove the tidal volume dependence. However, the normalization gives prominence to the relativity feature of the ventilation data. In other words, the ventilation change is relative after normalization. If ventilation gets better in some regions, there must be some regions where ventilation gets worse, since the total volume change in each data set must be the same tidal volume, or the total ventilation change over the whole lung must be zero between two normalized data sets. This

relativity feature is the reason that the FDV surface often shows symmetry with ventilation axis (Figure 4). Here is an easy example to help understanding the relativity feature. Assuming half of a uniformly ventilated lung becomes no ventilation (half A) and the other half is still uniformly ventilated (half B). After normalization, half A gets worse by 100% while half B gets better by 100% since half B is normalized to the tidal volume of before the change. Without normalization, the comparison would really depend on how deep the subject breathes (tidal volume dependence).

To spare functional lung volumes in treatment planning for SBRT, an objective or constraint thus is suggested that good ventilation regions derived from the pre-treatment 4D-CT should avoid radiation dose of higher than 20 Gy, based on this study.

Based on the linear-quadratic model, the biological effective dose (BED) of 4 Gy × 5 fractions = 20 Gy isodose line in the normal lung tissue is the same of 35 Gy isodose line in the conventional treatment of the prescription dose 2 Gy × 35 fractions = 70 Gy, and the 30 Gy isodose line in the SBRT is equivalent to 58 Gy isodose line in the conventional treatment. In the above calculation, the α/β ratio for the normal lung tissue is set at 3.1 Gy (Dubray *et al.*, 1995). The analysis on the 20 and 30 Gy dose levels thus can be applied to the conventional treatment at dose levels of 35 and 58 Gy.

A related study evaluated whether dose to the highly ventilated regions in the lung resulted in increased incidence of clinical toxicity, in which only the pre-RT 4D-CT was used for each patient to generate ventilation distribution and dose-ventilation histogram (Vinogradskiy et al., 2013). By comparison, our study used two sets of 4D-CT, one pre-RT and the other one post-RT, for each patient to directly calculate dose-induced ventilation change, which generated more statistically significant results.

For each case, there are two calculated ventilation data sets. The DSC is a measure of the similarity between the two data sets. The DSC data showed that there are some changes between the two data sets. The ventilation changes mostly are because of the radiation therapy treatments. However, the errors introduced in ventilation calculation may cause some ventilation variation. Although the reproducibility of ventilation derived from 4D-CT has been shown good in some studies (Du et al., 2013; Du et al., 2012), and the comparison between this method and other standard modality is good (Ding et al., 2012), some other studies also show that the ventilation calculation depends on DIR algorithm and ventilation calculation algorithm (Latifi et al., 2013a). The reason for the dependence is deemed that different algorithms handle 4D-CT artifacts differently.

Artifacts in 4D-CT could cause errors in DIR (Zhang et al., 2008), which in turn introduces errors in the derived ventilation data. To minimize the errors introduced by artifacts in 4D-CT, data sets with obvious mushroom artifacts in the diaphragm region, which are usually caused by irregular diaphragm motion, were excluded in this study. Since this is a retrospective study, this kind of exclusion would cause exclusion of clinical cases. If this method is used in a prospective study, timely review the 4D-CT data before the patient getting off the table is recommended. If obvious mushroom artifacts are present, re-scan with a slower respiration should be performed.

Quantum noise is another source of DIR errors. High quality 4D-CT is essential for accurate ventilation data (Latifi et al., 2013b).

5 CONCLUSIONS

Lung ventilation prior to and following radiotherapy can be measured using 4D-CT and DIR techniques. Changes in ventilation were observed with a correlation between ventilation change and radiation dose of greater than 20 Gy. These data suggest that ventilation calculated from 4D-CT may be a reliable tool for measuring/predicting the effects of dose on ventilation. Incorporating 4D-CT calculated ventilation in treatment planning would aid in avoiding well ventilated regions and possibly preventing lung injury.

ACKNOWLEDGEMENTS

This work was partially supported by a research grant from Varian Medical Systems, Inc., Palo Alto, CA. We thank Kenneth Forster for his involvement in the early stages in this project.

REFERENCES

Castillo R., Castillo E., Martinez J., and Guerrero T, 2010 Ventilation from four-dimensional computed tomography: density versus Jacobian methods *Phys Med Biol* 55 4661-85.

Dice L. R. 1945 Measures of the amount of ecologic association between species *Ecology* 26 297-302.

Ding K., Bayouth J. E., Buatti J. M., Christensen G E and Reinhardt J M 2010 4DCT-based measurement of changes in pulmonary function following a course of radiation therapy *Med Phys* 37 1261-72.

Ding K., Cao K., Fuld M. K., Du K., Christensen G. E., Hoffman E. A. and Reinhardt J. M. 2012 Comparison of image registration based measures of regional lung ventilation from dynamic spiral CT with Xe-CT *Med Phys* 39 5084-98.

Du K., Bayouth J. E., Cao K., Christensen G. E., Ding K. and Reinhardt J. M. 2012 Reproducibility of registration-based measures of lung tissue expansion *Med Phys* 39 1595-608.

Du K., Bayouth J. E., Ding K., Christensen G. E., Cao K. and Reinhardt J. M. 2013 Reproducibility of intensity-based estimates of lung ventilation *Med Phys* 40 063504.

Dubray B., Henry-Amar M., Meerwaldt J. H., Noordijk E. M., Dixon D. O., Cosset J-M and Thames H. D. 1995 Radiation-induced lung damage after thoracic irradiation for Hodgkin's disease: the role of fractionation *Radiother Oncol* 36 211-7.

Guerrero T., Sanders K., Noyola-Martinez J., Castillo E., Zhang Y., Tapia R., Guerra R., Borghero Y. and Komaki R. 2005 Quantification of regional ventilation from treatment planning CT *int J Radiat Oncol Biol Phys* 62 630-4.

Janssens G., de Xivry J. O., Fekkes S., Dekker A., Macq B., Lambin P. and van Elmpt W. 2009 Evaluation of nonrigid registration models for interfraction dose accumulation in radiotherapy *Med Phys* 36 4268-76.

Latifi K., Forster K. M., Hoffe S. E., Dilling T. J., Elmpt W. v., Dekker A. and Zhang G. G. 2013a Dependence of ventilation image derived from 4D CT on deformable image registration and ventilation algorithms *J Appl Clin Med Phy* 14 150-62.

Latifi K., Huang T-C, Feygelman V., Budzevich M. M., Moros E. G., Dilling T. J., Stevens C. W., Elmpt W. v., Dekker A. and Zhang G. G. 2013b Effects of quantum noise in 4D-CT on deformable image registration and derived ventilation data *Phys Med Biol* 58 7661-72.

Latifi K., Zhang G., Stawicki M., van Elmpt W., Dekker A. and Forster K. 2013c Validation of three deformable image registration algorithms for the thorax *J Appl Clin Med Phys* 14 19-30.

Lavrenkov K., Christian J. A., Partridge M., Niotsikou E., Cook G., Parker M., Bedford J. L. and Brada M. 2007 A potential to reduce pulmonary toxicity: the use of perfusion SPECT with IMRT for functional lung avoidance in radiotherapy of non-small cell lung cancer *Radiother Oncol* 83 156-62.

Loring S. H., Brown R. E., Gouldstone A. and Butler J. P. 2005 Lubrication regimes in mesothelial sliding *J. Biomech.* 38 2390-6.

Petersson J., Sánchez-Crespo A., Rohdin M., Montmerle S., Nyrén S., Jacobsson H., Larsson S. A., Lindahl S. G. E., Linnarsson D., Glenny R. W. and Mure M. 2004 Physiological evaluation of a new quantitative SPECT method measuring regional ventilation and perfusion *J Appl Phisiol* 96 1127-36.

Reinhardt J. M., Ding K., Cao K., Christensen G. E., Hoffman E. A. and Bodas S. V. 2008 Registration-based estimates of local lung tissue expansion compared to xenon CT measures of specific ventilation *Med. Image Anal.* 12 752-63.

Shioyama Y., Jang S. Y., Liu H. H., Guerrero T., Wang X., Gayed I. W., Erwin W. D., Liao Z., Chang J. Y., Jeter M., Yaremko B. P., Borghero Y. O., Cox J. D., Komaki R. and Mohan R. 2007 Preserving functional lung using perfusion imaging and intensity-modulated radiation therapy for advanced-stage non–small cell lung cancer *Int J Radiat Oncol Biol Phys* 68 1349-58.

Simon B. A. 2000 Non-invasive imaging of regional lung function using X-ray computed tomography *J Clin Monitoring Computing* 16 433-42.

Suga K. 2002 Technical and analytical advances in pulmonary ventilation SPECT with Xenon-133 gas and Tc-99m-Technegas *Ann. Nucl. Med.* 16 303-10.

Vinogradskiy Y., Castillo R., Castillo E., Tucker S. L., Liao Z., Guerrero T. and Martel M. K. 2013 Use of 4-dimensional computed tomography-based ventilation imaging to correlate lung dose and function with clinical outcomes *Int J Radiat Oncol Biol Phys* 86 366-71.

Yaremko B. P., Guerrero T. M., Noyola-Martinez J., Guerra R., Lege D. G., Nguyen L. T., Balter P. A., Cox J. D. and Komaki R. 2007 Reduction of normal lung irradiation in locally advanced non-small-cell lung cancer patients, using ventilation images for functional avoidance *Int J Radiat Oncol Biol Phys* 68 562-71.

Zhang G., Huang T-C, Dilling T., Stevens C. and Forster K. 2011 Comments on 'Ventilation from four-dimensional computed tomography: density versus Jacobian methods' *Phys Med Biol* 56 3445-6.

Zhang G., Huang T-C, Guerrero T., Lin K-P, Stevens C., Starkschall G. and Forster K. 2008 Use of three-dimensional (3D) optical flow method in mapping 3D anatomic structure and tumor contours across four-dimensional computed tomography data *J Appl Clin Med Phy* 9 59-69.

Zhang G. G., Huang T. C., Dilling T., Stevens C. and Forster K. M. 2009 Derivation of high-resolution pulmonary ventilation using local volume change in four-dimensional CT data. In: *World Congress on Medical Physics and Biomedical Engineering,* ed O Dössel and W C Schlegel (Munich, Germany: Springer) pp 1834-7.